

# Critical behavior in Ricci flow

David Garfinkle \*

Department of Physics, Oakland University  
Rochester, Michigan 48309

James Isenberg †

Department of Mathematics, University of Oregon  
Eugene, OR

December 24, 2021

## Abstract

We use numerical techniques to study the formation of singularities in Ricci flow. Comparing the Ricci flows corresponding to a one parameter family of initial geometries on  $S^3$  with varying amounts of  $S^2$  neck pinching, we find critical behavior at the threshold of singularity formation

## 1 Introduction

Given a manifold  $M^n$  and a Riemannian metric  $\bar{g}$  specified on  $M^n$ , the Ricci flow determines a one parameter family of metrics  $g(t)$  via the geometric evolution equation

$$\partial_t g_{ab}(t) = -2R_{ab}[g(t)], \quad (1)$$

with initial condition

$$g(0) = \bar{g}. \quad (2)$$

---

\*Email: garfinkl@oakland.edu

†Email: jim@newton.uoregon.edu

(Here  $R_{ab}$  is the Ricci tensor of the metric  $g_{ab}$ .) Ricci flow has been a very effective tool for studying the sorts of special geometries which a manifold admits. In most of these applications to date [6] [5] [7], the flow is shown to converge to the special geometries (e.g., to a constant negative curvature hyperbolic metric for the Ricci flow on any two dimensional manifold of genus greater than one). Future applications, however, are likely to require that one understand Ricci flows which develop singularities.

In this work, we begin a program of numerical study of Ricci flow singularities. We focus here on the following question: Say we have a one parameter family of metrics  $\bar{g}_\lambda$  specified on the manifold  $S^3$  and say we know that the Ricci flows  $g_\lambda(t)$  starting at  $\bar{g}_\lambda$  for very large  $\lambda$  converge (with the volume suitably normalized) to the round sphere metric, while the Ricci flows  $g_\lambda(t)$  for small values of the parameter  $\lambda$  become singular, in the sense that (regardless of volume norm) the curvature of  $g_\lambda(t)$  grows without bound as  $t$  increases. What happens to the Ricci flows  $g_\lambda(t)$  with intermediate values of  $\lambda$ ? Is there, in particular, a certain threshold value  $\lambda_{crit}$  for which the Ricci flow has interesting intermediate behavior: neither convergence, nor formation of a standard singularity?

For solutions of Einstein's equations representing gravitational collapse, this sort of question has been studied extensively [1] [4]. Very distinct threshold behavior has been found, with a remarkable degree of universality. That is, in examining a number of one parameter families of initial data for gravitational collapse, one finds qualitatively the same sort of discretely self-similar solution occurring for threshold initial data for all of these families.

For Ricci flow, our work here is the first search for critical behavior. We have examined a particular one parameter family of spherically symmetric "corseted sphere" geometries on  $S^3$ , with the parameter describing the degree of corseting at the equator, and therefore parametrizing the magnitude of the  $S^2$  neck pinch curvature at the equator. We do indeed find numerically that for geometries with a small amount of corseting, the Ricci flow converges to the round sphere metric, while for geometries with a large amount of corseting, an  $S^2$  neck pinch singularity occurs. Moreover, we find that there is a critical value of the parameter, dividing the two regimes. Finally, our studies show that the Ricci flow for the geometry marked by the critical parameter value neither converges to the round sphere geometry nor forms an  $S^2$  neck pinch singularity. Instead, this flow approaches a "javelin" geometry, marked by curvature singularities at the poles, with roughly uniform curvature between the poles. This javelin geometry corresponds to the "type 3"

singularity described by Hamilton [8] and discussed by Chow.[2]

We describe in detail in Section 2 the corseted sphere geometries that we study here, and write out the detailed form of the Ricci flow equations for these geometries. Also in Section 2 we describe our numerical methods. We present our results in Section 3, noting the behavior of the Ricci flows for subcritical, supercritical, and critical initial geometries. Concluding remarks appear in Section 4.

## 2 Corseted Sphere Geometries and Their Flow Equations

The corseted sphere geometries and their flows are all represented by spherically symmetric metrics on  $S^3$  of the form

$$g = e^{2X} \left( e^{-2W} d\psi^2 + e^{2W} \sin^2\psi [d\theta^2 + \sin^2\theta d\phi^2] \right) \quad (3)$$

Here  $(\psi, \theta, \phi)$  are standard angular coordinates on the three sphere; spherical symmetry holds so long as we assume that the metric functions  $X$  and  $W$  are functions only of  $\psi$ .

Smoothness of the metric at the poles, where  $\psi$  takes the values 0 and  $\pi$ , requires that  $X$  and  $W$  be even functions of  $\sin\psi$  in a neighborhood of the poles. Therefore  $\partial_\psi X$  and  $\partial_\psi W$  must vanish at the poles. However, smoothness of the metric also requires that  $W$  vanish at the poles. To avoid the numerically awkward imposition of two conditions on  $W$  at a single point, it is convenient to replace the variable  $W$  by  $S \equiv W/\sin^2\psi$ . Smoothness of the metric at the poles can then be enforced by the requirement that  $\partial_\psi X$  and  $\partial_\psi S$  vanish at  $\psi = 0$  and  $\psi = \pi$ .

To obtain the corseted sphere geometries, we set  $W = X$ , and choose  $X$  so that  $4e^{4X}\sin^2\psi = \sin^2 2\psi$  for  $\cos^2\psi \geq 1/2$  and  $4e^{4X}\sin^2\psi = \sin^2 2\psi + 4\lambda\cos^2 2\psi$  for  $\cos^2\psi \leq 1/2$ . Here  $\lambda$  is a constant, which parametrizes the degree of corseting for these geometries. For  $\lambda = 0$ , the geometry represents two round three spheres joined at the poles. This is a singular geometry. For  $\lambda$  positive, the cusp smooths out and the geometry is non singular; however, for small values of  $\lambda$  one still expects the curvature at the tightly pinched equator to be very large. In Figure 1, we graph the area of the  $\psi = \text{constant}$  cross-sections as a function of  $\psi$  for a few representative values of  $\lambda$ . In Figure 2, we graph the Ricci curvature eigenvalue in the direction along the  $S^2$  symmetry

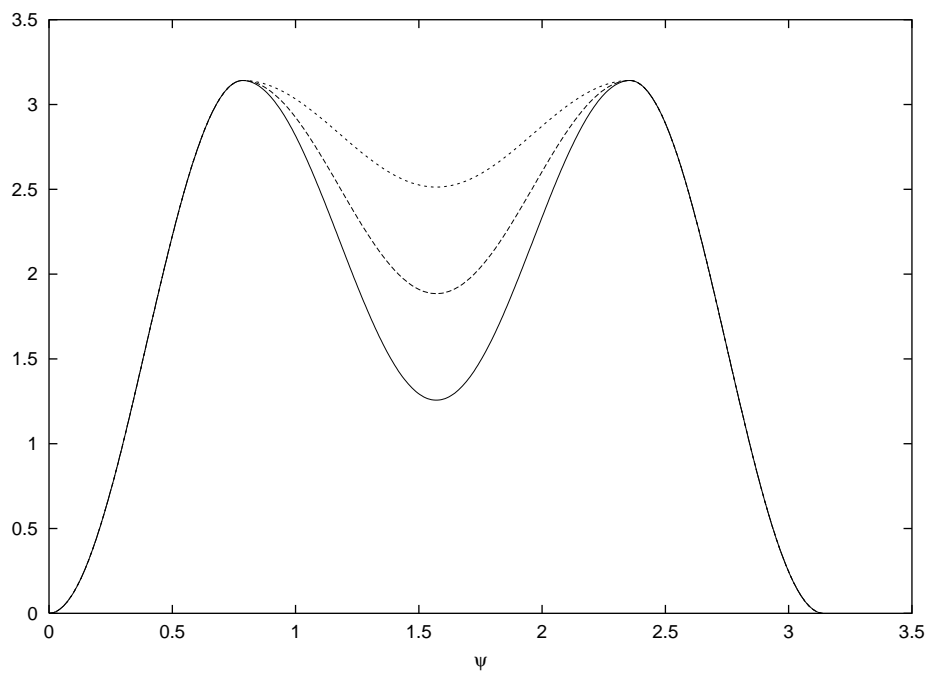


Figure 1: area of the  $S^2$ s as a function of  $\psi$  for  $\lambda = 0.1$  (solid line),  $\lambda = 0.15$  (dashed line) and  $\lambda = 0.2$  (dotted line).

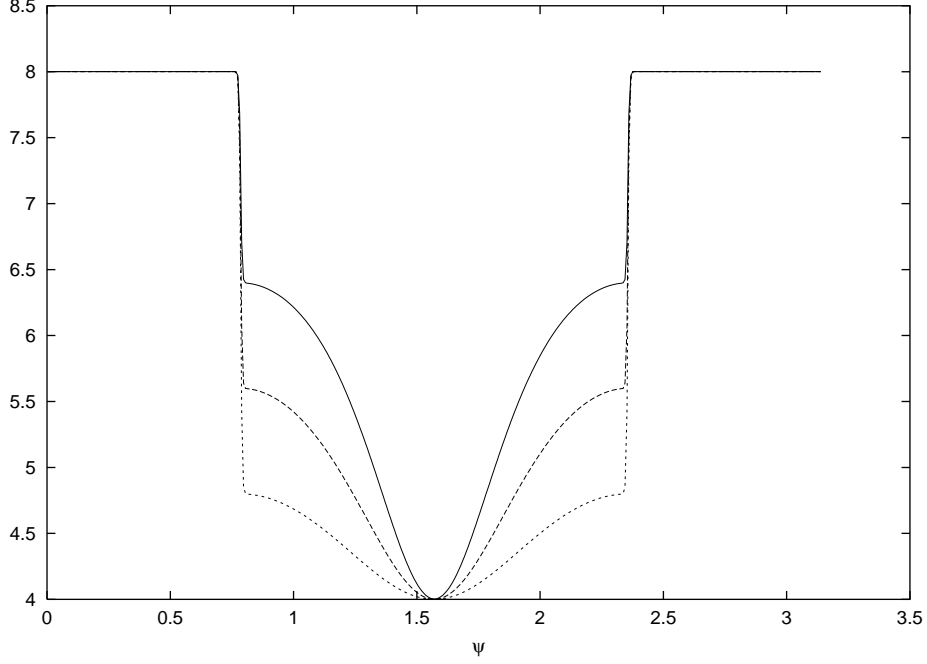


Figure 2:  $R_{S^2}$  as a function of  $\psi$  for  $\lambda = 0.1$  (solid line),  $\lambda = 0.15$  (dashed line) and  $\lambda = 0.2$  (dotted line).

as a function of  $\psi$ . Note that as a consequence of the assumption in these geometries that  $W = X$ , we verify that the coordinate  $\psi$  gives the value of the geodesic distance in the radial direction.

We are interested in the Ricci flow of the corseted sphere metrics. However, since the Ricci flow equation (1) is only weakly parabolic, and since numerical evolutions appear to be more stable for strongly parabolic systems, we instead work with the DeTurck flow. [3] The strongly parabolic PDE system generating the DeTurck flow is

$$\partial_t \hat{g}_{ab} = -2\hat{R}_{ab} + 2\hat{D}_{(a}V_{b)} \quad (4)$$

where  $\hat{D}_a$  is the derivative operator associated with the metric  $\hat{g}_{ab}$ , and where the vector field  $V^a$  is given by

$$V^a = \hat{g}^{bc} (\hat{\Gamma}_{bc}^a - \Delta_{bc}^a) \quad (5)$$

with  $\hat{\Gamma}_{bc}^a$  being the connection of the metric  $\hat{g}_{ab}$  and with  $\Delta_{bc}^a$  being any fixed connection. For a given initial geometry, one can find the corresponding

Ricci flow  $g(t)$  by first finding the corresponding DeTurck flow  $\hat{g}_{ab}$ , and then pulling back via the time dependent diffeomorphism generated by the vector field  $V$  defined above.

Note that neither the Ricci flow (1) nor the DeTurck flow (4) preserves volume. One can normalize the volume for either of the flows by adding the term  $\frac{2\hat{r}}{3} \hat{g}_{ab}$ , with  $\hat{r}$  the spatial average of the scalar curvature, to the flow equation. Alternatively, one can control the volume along either flow by periodic uniform blowups.

We now calculate the volume normalized DeTurck flow for spherically symmetric metrics of the form (3). Choosing the reference connection to be that of the round sphere, and using primes to denote the spatial derivative  $\partial_\psi$ , we obtain the evolution equations

$$\begin{aligned} \partial_t X = e^{2(W-X)} & \left[ X'' + 2 \cot \psi X' - 2 + \frac{1}{2}([X']^2 + [W']^2) + 3X'W' \right. \\ & \left. + (1 - e^{-4W}) \left( \frac{1}{2\sin^2 \psi} + 1 + 2 \cot \psi W' \right) \right] + \frac{\hat{r}}{3}. \end{aligned} \quad (6)$$

$$\begin{aligned} \partial_t W = e^{2(W-X)} & \left[ W'' + 2 \cot \psi W' - \frac{1}{2}([X']^2 + [W']^2) - 3X'W' \right. \\ & \left. + (1 - e^{-4W}) \left( 1 - \frac{3}{2\sin^2 \psi} - 2 \cot \psi [X' + 2W'] \right) \right]. \end{aligned} \quad (7)$$

Here we note that the average scalar curvature  $\hat{r}$  is given by

$$\hat{r} = \frac{2}{N} \int_0^\pi d\psi e^{X+3W} \left( e^{-4W} - 1 - 4 \sin \psi \cos \psi W' + \sin^2 \psi [3 + (X' + W')^2] \right), \quad (8)$$

where the normalization constant  $N$  is given by

$$N \equiv \int_0^\pi d\psi e^{3X+W} \sin^2 \psi. \quad (9)$$

We also note that the only non vanishing component of the vector field  $V$  defined in (5) is

$$V_\psi = -1 \left( 3W' + X' + 2 \cot \psi [1 - e^{-4W}] \right) \quad (10)$$

As discussed earlier, it is useful to work with the quantity  $S \equiv W/\sin^2 \psi$ , rather than  $W$ . Since this definition implies that  $W' = \sin^2 \psi S' + 2 \sin \psi \cos \psi S$ ,

we readily obtain

$$\begin{aligned} \partial_t S = e^{2(W-X)} & \left[ S'' + 6 \cot \psi S' - 8S - \frac{3}{2\sin^4 \psi} (1 - 4W - e^{-4W}) \right. \\ & \left. + \frac{1 - e^{-4W}}{\sin^2 \psi} (1 - 2[\cot \psi X' + 2 \sin \psi \cos \psi S' + 4\cos^2 \psi S]) \right. \\ & \left. - \frac{1}{2} ([X'/\sin \psi]^2 + [\sin \psi S' + 2 \cos \psi S]^2 + 6[X'/\sin \psi][\sin \psi S' + 2 \cos \psi S]) \right]. \end{aligned} \quad (11)$$

Equations (6) and (11) are the ones that we evolve numerically, noting that wherever we encounter  $W$  or  $\partial_\psi W$  these are to be expressed in terms of  $S$  and  $\partial_\psi S$ .

### 3 Numerical Results

To study these evolution equations numerically, we proceed as follows: We divide the spatial coordinate range  $(0, \pi)$  of  $\psi$  into  $N - 2$  pieces, so that we have  $\Delta\psi = \pi/(N - 2)$ . We choose  $N$  grid points, including a pair which run outside the coordinate range. So the first spatial grid point is at  $\psi = -\Delta\psi/2$ , while the last is at  $\psi = \pi + \Delta\psi/2$ . Then a function of the form  $F(\psi, t_0)$  for fixed time  $t_0$  is replaced by a set of  $N$  numbers  $F_i = F((i - \frac{3}{2})\Delta\psi, t_0)$  where  $1 \leq i \leq N$ . Spatial derivatives are replaced by centered finite differences in the following way:

$$\partial_\psi F \rightarrow \frac{F_{i+1} - F_{i-1}}{2\Delta\psi} \quad (12)$$

$$\partial_\psi \partial_\psi F \rightarrow \frac{F_{i+1} + F_{i-1} - 2F_i}{(\Delta\psi)^2} \quad (13)$$

For the time dependence of these functions, we choose a fixed time step  $\Delta t$ , and replace  $F((i - \frac{3}{2})\Delta\psi, n\Delta t)$  by the numbers  $F_i^n$ .

Now, for an evolution equation of the form  $\partial_t F(\psi, t) = G(\psi, t)$  we numerically evolve using the approximation

$$F_i^{n+1} = F_i^n + \Delta t G_i^n \quad (14)$$

This evolution is implemented for all values of  $i$  except 1 and  $N$ . Note that these two “ghost zones” are not part of the manifold since  $\psi$  is not in the range  $0 \leq \psi \leq \pi$ . At the ghost zones we use smoothness of the metric which

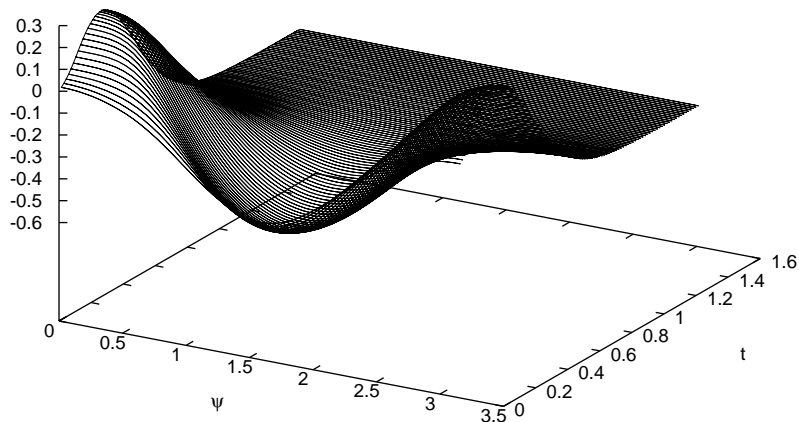


Figure 3:  $X$  for subcritical Ricci flow

implies that  $X'$  and  $S'$  vanish at the poles. We implement this condition as  $X_1 = X_2$  and  $X_N = X_{N-1}$  (and correspondingly for  $S$ ).

Runs were done (on Unix and Linux workstations), starting from a wide range of initial corseted sphere geometries (parametrized by  $\lambda$ ). As noted above, for small  $\lambda$  we expect that the geometry is sufficiently close to singular that the distorted  $S^3$  will pinch off into a singularity, while for sufficiently large  $\lambda$  the flow may overcome the distortion to evolve the data to a single round  $S^3$ .

These expectations are confirmed by our numerical simulations. Figures 3 and 4 show the results of a “subcritical” run, *i.e.* one which does not result in a singularity. For this run we have chosen  $\lambda = 0.2$ . Note that at late times we find that  $X$  approaches a constant and that  $S \rightarrow 0$ . These are the values for a round  $S^3$ .

Rather than focusing on the evolution of the metric components, it is more instructive to examine the behavior of curvature. As a consequence of the spherical symmetry of the geometries, the Ricci tensor  $R^a_b$  has two independent eigenvalues. We call these eigenvalues  $R_{S^2}$  and  $R_\perp$  where  $R_{S^2}$



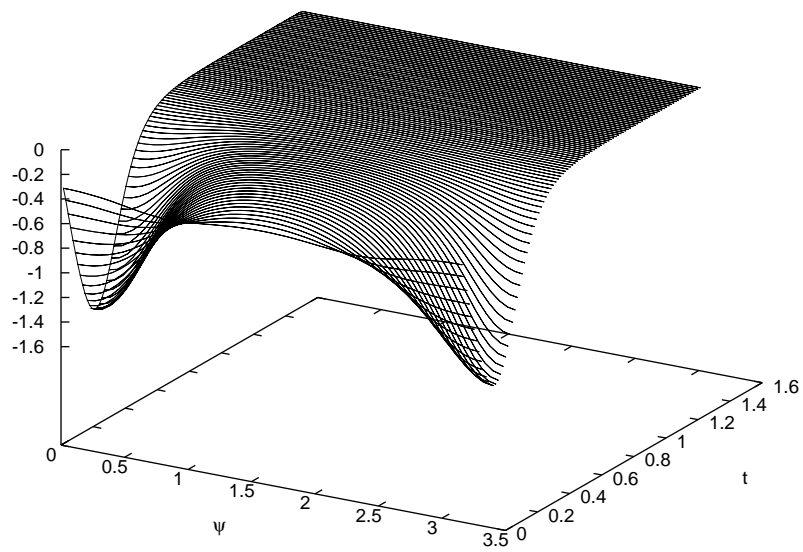


Figure 4:  $S$  for subcritical Ricci flow

corresponds to the eigenspace in the symmetry  $S^2$  directions and  $R_\perp$  corresponds to the eigenspace orthogonal to the symmetry  $S^2$  directions. Some straightforward calculations show

$$R_\perp = -2e^{2(W-X)} [-1 + X'' + W'' + (X' + 3W') \cot \psi + 2(X' + W')W'] \quad (15)$$

$$R_{S^2} = -e^{2(W-X)} \left[ -2 + \frac{1 - e^{-4W}}{\sin^2 \psi} + X'' + W'' + (3X' + 5W') \cot \psi + (X' + W')(X' + 3W') \right] \quad (16)$$

(where we note that  $W, W'$  and  $W''$  can be expressed in terms of  $S, S'$  and  $S''$ ). One can express the invariants of the Ricci tensor (and since we are in 3 dimensions, the invariants of the Riemann tensor as well) in terms of  $R_{S^2}$  and  $R_\perp$ . We have

$$R = 2R_{S^2} + R_\perp \quad (17)$$

$$R^{ab}R_{ab} = 2R_{S^2}^2 + R_\perp^2 \quad (18)$$

$$R^{abcd}R_{abcd} = 4R^{ab}R_{ab} - R^2 = 2R_\perp^2 + (R_\perp - 2R_{S^2})^2 \quad (19)$$

Figures 5 and 6 show the behavior of  $R_{S^2}$  and  $R_\perp$  for the same subcritical run. Note that both eigenvalues asymptotically approach the same constant value at late times, which confirms the contention that the flow of a subcritical geometry converges to the round sphere geometry.

We next consider the DeTurck flow of “supercritical” initial geometries, *i.e.* those for which the evolution is singular. Figures 7 and 8 plot the behavior of  $R_{S^2}$  and  $R_\perp$  for an initial geometry with  $\lambda = 0.11$ . Characteristically, we find that in the neighborhood of the equator,  $R_{S^2}$  grows without bound as  $t$  increases, while  $R_\perp$  appears to stay bounded. As well, both are bounded away from the equator. This signals the formation of an  $S^2$  neck pinch singularity at the equator.

The behavior just described for the DeTurck flow—and consequently for the Ricci flow—for  $\lambda = 0.11$  corseted sphere data is also found for any initial geometry with  $\lambda < 0.11$ . Similarly, for  $\lambda > 0.2$ , the flow has the subcritical behavior illustrated in Figures 5 and 6. This has led us to seek critical behavior at a threshold value. Using a binary search, we have located the threshold value at approximately  $\lambda = 0.1639$ .

The DeTurck flow starting at a corseted sphere geometry with this value of  $\lambda$  behaves differently than the flow for both subcritical and supercritical

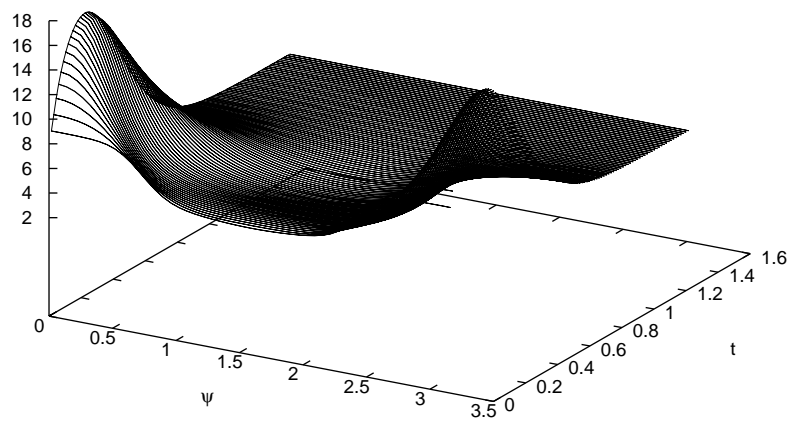


Figure 5:  $R_{S^2}$  for subcritical Ricci flow

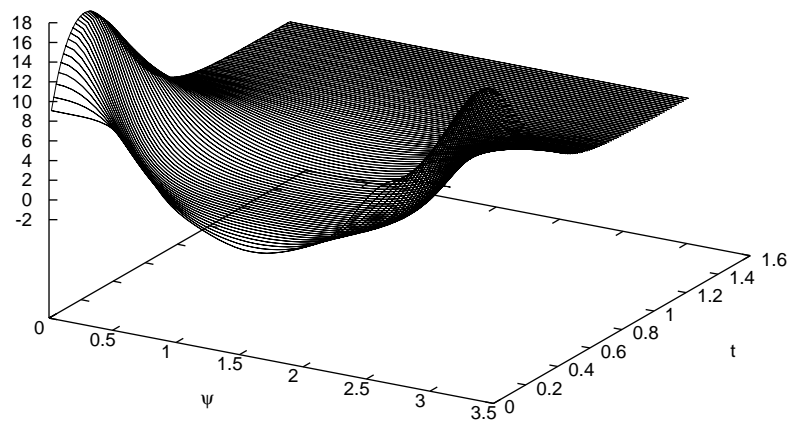


Figure 6:  $R_{\perp}$  for subcritical Ricci flow

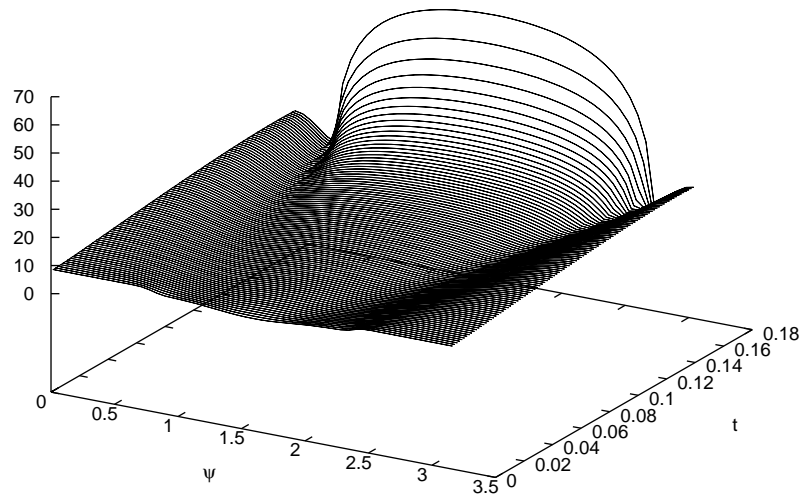


Figure 7:  $R_{S^2}$  for supercritical Ricci flow

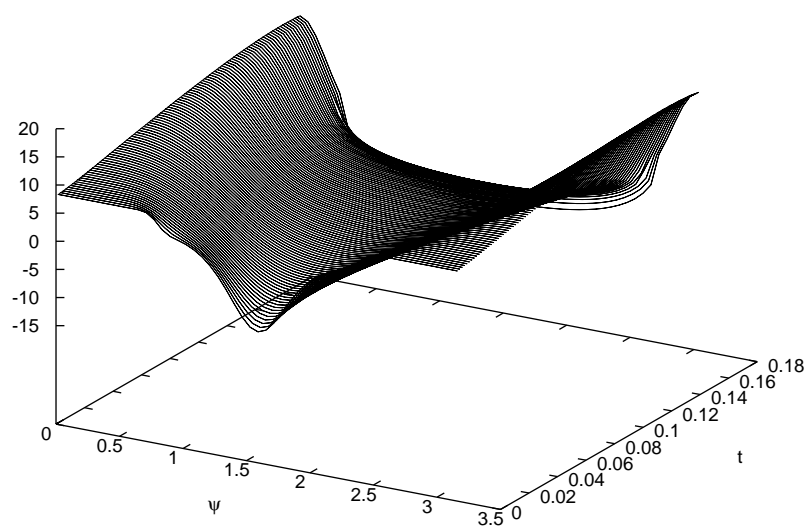


Figure 8:  $R_{\perp}$  for supercritical Ricci flow

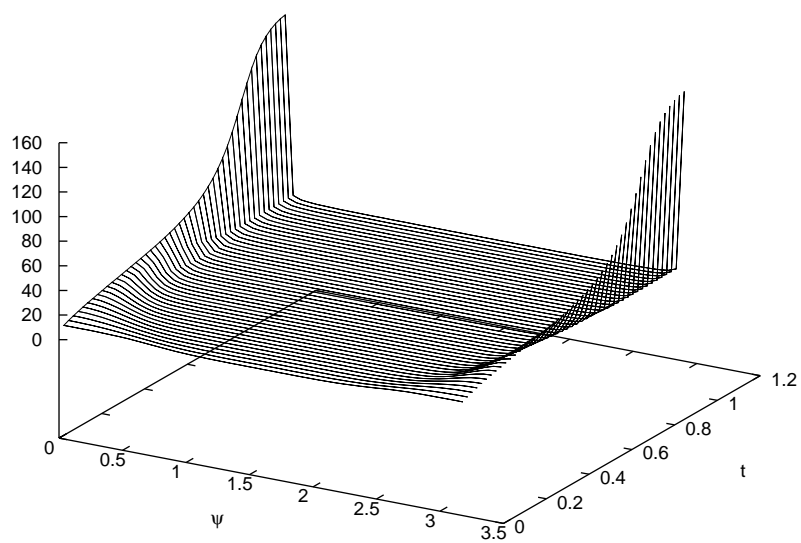


Figure 9:  $R_{S^2}$  for critical Ricci flow

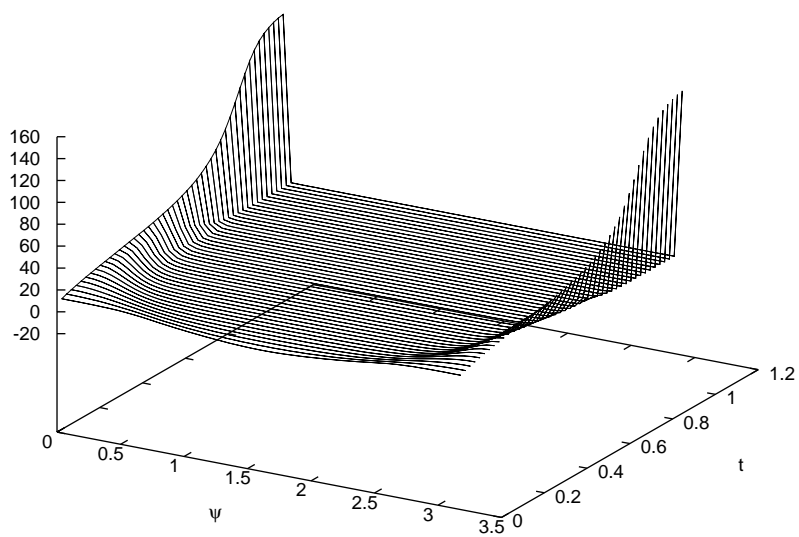


Figure 10:  $R_{\perp}$  for critical Ricci flow



geometries. As seen in Figures 9 and 10,  $R_{\perp}$  gets small everywhere except at the poles, while  $R_{S^2}$  slowly grows everywhere except at the poles. At the poles, both curvatures get very large. In a sense, the geometry approaches that of a three dimensional javelin, with  $S^2$  cross-sections.

## 4 Conclusions

The numerical work we have described here clearly shows rather special behavior for the Ricci flow at the threshold parameter value for a one parameter family of corseted spheres. Is this behavior in any sense universal? This has not yet been determined. We plan to examine other families of initial geometries to see if the threshold behavior persists. One interesting set of geometries we plan to examine are those with, initially, more than one neck pinch.. Do the neck pinches coalesce? Do we get javelin geometries for threshold initial data? We also plan to consider families of initial data which are not spherically symmetric.

## 5 Acknowledgments

This work was partially supported by NSF grants PHY-9988790 to Oakland University and PHY-0099373 to The University of Oregon. We also thank the University of California at San Diego for hospitality while some of this work was carried out.

## References

- [1] M. Choptuik, *Universality and Scaling in the Gravitational Collapse of a Massless Scalar Field*, Phys. Rev. Lett. **70**, (1993) 9-12
- [2] B. Chow, *A Survey of Hamilton's Program for the Ricci Flow on 3-Manifolds*, preprint DG/0211266
- [3] D. DeTurck, *Deforming Metrics in the Direction of their Ricci Tensor*, J. Differential Geom. **18**, (1983) 157-162
- [4] C. Gundlach, *Critical Phenomena in Gravitational Collapse* Phys. Rept. **376**, (2003) 339-405

- [5] R.S. Hamilton, *The Ricci Flow on Surfaces*, in *Mathematics and General Relativity*, AMS Contemporary Mathematics **71** (1988) 237-262
- [6] R.S. Hamilton, *Three-Manifolds with Positive Ricci Curvature*, J. Differential Geom. **17**, (1982) 255-306
- [7] R.S. Hamilton, *Four-Manifolds with Positive Curvature Operator*, J. Differential Geom. **24**, (1986) 153-179
- [8] R.S. Hamilton, *The Formation of Singularities in the Ricci Flow*, Surveys in Diff. Geom. **2**, (1995) International Press 7-136